ISBN: 978-628-96613-3-0. ISSN: 2414-6390. Digital Object Identifier: https://dx.doi.org/10.18687/LACCEI2026.1.1.1490

Design and Structural Analysis of an Electric Vehicle Chassis Using the Finite Element Method

Mijael Ramos Puma[1]; Waldir Huacarpuma Huamani[2]; Rodrigo Mamani Quispe[3]; Ridward Berrospi Peñaloza[4]; Arturo Velasquez Cruz[5]
[1,2,3,4,5]Universidad Tecnológica del Perú, Perú, [1] *U21210005@utp.edu.pe*, [2]*U19209295@utp.edu.pe*,[3] *U21217472@utp.edu.pe* [4]*U20207197@utp.edu.pe*, [5] *C25661@utp.edu.pe*,

Abstract*– This study presents the structural design and analysis of a chassis for a compact electric vehicle using the Finite Element Method (FEM). The chassis was modeled in Autodesk Inventor and evaluated through static simulations in ANSYS under four scenarios: full load with all wheels on the ground, asymmetric loading with one front wheel suspended, one rear wheel suspended, and emergency braking. Results show that under full load, the maximum displacement was 0.575 mm, indicating high stiffness. The most critical deformation occurred with a suspended front wheel, reaching 3.2336 mm, while emergency braking generated the peak stress of 136.04 MPa, remaining well below the yield strength of structural steel. These findings confirm that even under extreme conditions, the chassis operates within the elastic range. Material comparison revealed distinct behaviors. Structural steel and Q345 exhibited similar stiffness and strength, limiting displacement to 3.2336 mm under torsional load and maintaining stresses of 136 MPa during braking. Aluminum, in contrast, offered significant weight reduction but showed greater flexibility, with displacements up to 9.84139 mm and stresses limited to 44.699 MPa, suggesting its viability only with geometric reinforcement. Overall, the proposed chassis design meets safety and performance requirements across all scenarios. The study also identifies improvement opportunities through localized reinforcement and geometric optimization—such as increasing thickness in high-stress regions or replacing rectangular profiles with circular sections without significantly increasing weight. These results provide a foundation for future optimization and dynamic analysis, supporting the development of lightweight, efficient, and structurally robust electric vehicle platforms.

Keywords-- Finite Element Method , Electric Vehicle Chassis, Structural Analysis, Lightweight Design

I. INTRODUCTION

The structural design of a vehicle chassis represents a central challenge in modern engineering, particularly in applications requiring an optimal balance between stiffness, mechanical strength, and weight efficiency. These factors are crucial for improving performance, safety, and energy efficiency in electric vehicles and lightweight transportation platforms [14],[18]. In this context, the Finite Element Method (FEM) has become an essential tool for predicting structural behavior under static and dynamic loads prior to fabrication [1],[16], enabling the identification of critical stress regions and supporting more informed design decisions[19]. Several studies have demonstrated that topological optimization, dynamic analysis, and advanced structural evaluation can significantly enhance the configuration and robustness of chassis structures, contributing to more efficient use of materials such as steel and fiber-reinforced composites [9],[11],[12]. These advancements have also improved understanding of vibration, fatigue behavior, and torsional stiffness, which are key factors influencing chassis performance under real operating conditions [15],[20]. Furthermore, research in industrial and agricultural vehicles highlights the relevance of analyzing multiaxial loading, impact conditions, and irregular terrain, all of which impose complex demands on the structural system [3],[7]. The integration of CAD modeling with FEM simulations has enhanced the accuracy and efficiency of the chassis design process, enabling the development of lighter structures without compromising safety [2],[10]. Recent studies emphasize that the combined optimization of geometry, material, and structural performance leads to highly efficient chassis capable of withstanding extreme loading scenarios with reduced mass [9],[20]. Based on this context, the present work conducts a structural assessment of a steel chassis through linear static simulations under various load conditions to evaluate stiffness, stress distribution, and opportunities for design improvement.

II. METHODS

ESTABLISHMENT OF THE STRUCTURAL MODEL OF THE CHASSIS

In this study, the structural chassis of a light four-wheeled vehicle is analyzed to evaluate its mechanical behavior using the finite element method [18]. Based on established design criteria, the main dimensions of the model were defined as shown in Table I: 2150 mm in length, 1450 mm in width, and 320 mm in height. The chassis consists of a welded tubular structure constructed with 50 mm × 30 mm × 5 mm rectangular profiles, configured in a spatial arrangement that provides adequate torsional rigidity and bending strength. During the geometric modeling process, reasonable simplifications were applied to optimize the calculations and reduce the complexity of the analysis. Details such as weld points, fillets, mounting holes, and chamfers were not considered; these were replaced by straight joints and flat surfaces, maintaining the structural representativeness of the model without compromising the accuracy of the results. Following this procedure, the three-dimensional model of the chassis was generated in the INVENTOR software, as shown in Figure 1, resulting in a structure with an approximate weight of 50 kg. The material selected for the chassis is structural steel, chosen for its high strength-to-weight ratio, good machinability, and corrosion resistance [14]. The model was also analyzed in ANSYS, where the mesh was generated using solid tetrahedral elements. mesh convergence check was performed to ensure that the numerical results were not dependent on element size. The selected mesh provided a balance between computational efficiency and accuracy. Boundary conditions were defined by fixing the wheel contact regions and applying distributed loads based on component weights and inertial factors.

The chassis is considered to be subjected primarily to loads from its own weight, the propulsion system, the batteries, the suspension assembly, and the occupants. The mass values corresponding to each of these components are presented in Table II.

TABLE I
MAIN VEHICLE PARAMETERS

Chassis dimensions	2150 x 1450 x 320 mm
Dimensions of rectangular tubes	50 x 30 x 5 mm
Maximum battery life	300 km
Number of seats	2
Maximum speed	80 km/h

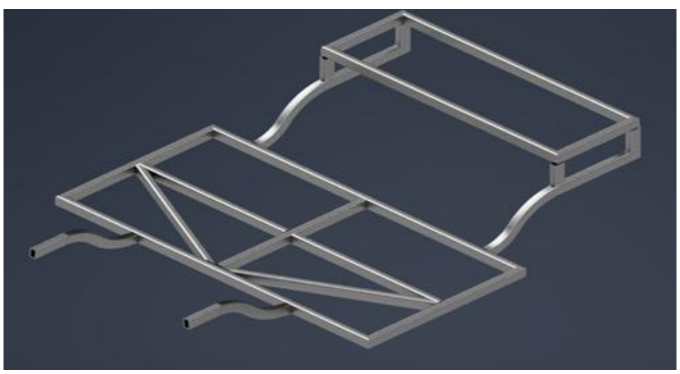

Fig. 1 General chassis structure.

TABLE II
PARAMETERS OF EACH COMPONENT

Name	Component weights (kg)	Amount
Electric machine	40	1
Battery pack	30	3
Suspension	30	4
Passengers	70	2

III. RESULTS

ANALYSIS OF CHASSIS STRESSES AND DEFORMATIONS

A. Static analysis of the chassis under full load condition

Under a fully loaded condition with all four wheels in contact with the ground, the main loads acting on the chassis structure come from the weight of the frame itself, the weight of mounted components such as the propulsion system, batteries, and suspension, as well as the total weight of the occupants. These loads were applied in a distributed manner over the corresponding areas of the model. The deformation diagram in Figure 2 shows that, under full load, the maximum chassis displacement is approximately 0.5754 mm, located in the rear of the structure, specifically in the beams supporting the components. Towards the front and center of the frame, the deformation gradually decreases, becoming negligible at the ends. The obtained value is well below the allowable deformation of the material; therefore, the structural rigidity of the chassis meets the established requirements.

Based on the equivalent stress diagram shown in Figure 3, a maximum value of approximately 45.099 MPa is reached, which is significantly lower than the material's yield strength. Therefore, the structural strength of the chassis is adequate, and the structure can operate safely under the considered loading conditions.

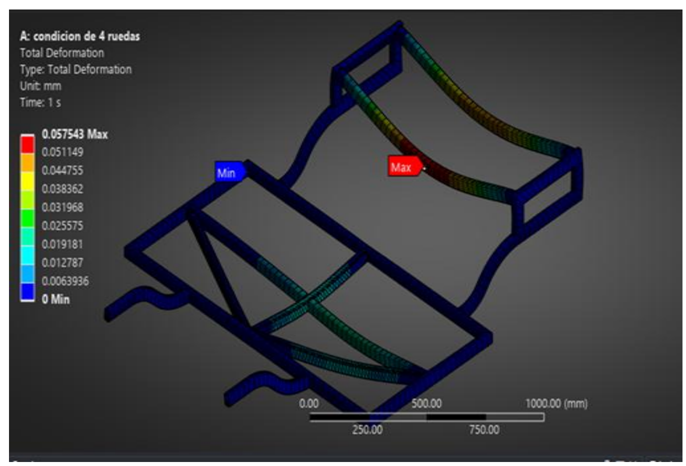

Fig. 2 Equivalent displacement diagram of the frame structure.

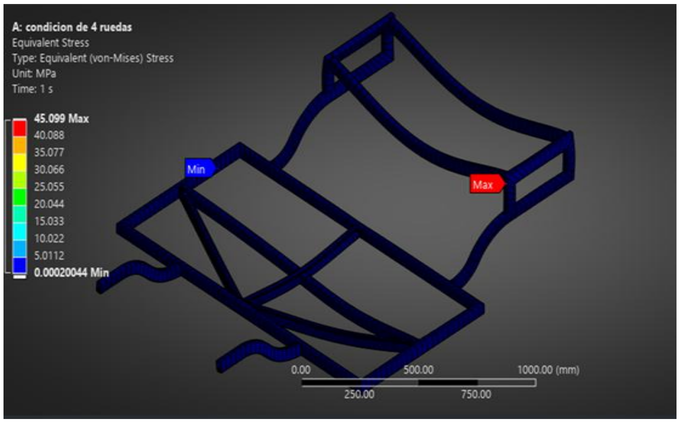

Fig. 3 Equivalent stress diagram (Von Mises).

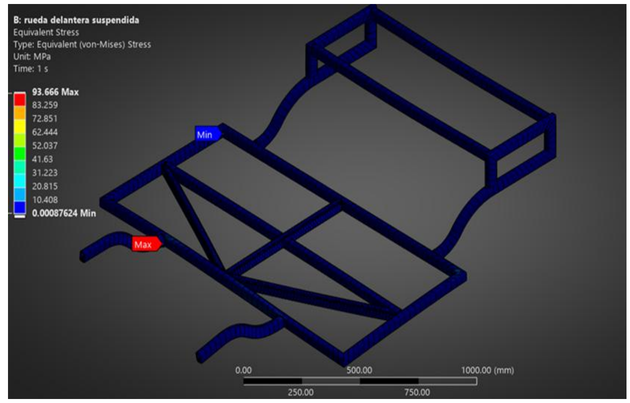

Fig. 5 Equivalent stress diagram (Von Mises).

C. Static analysis of the chassis where one side of the front wheel is suspended under full load

Under this condition, the structural behavior of the chassis was simulated when one of the front wheels was suspended, reproducing the effect of uneven terrain or a maneuver with uneven support. The total system load was considered, applying a dynamic factor of 1.3 to represent inertial effects.

The supports corresponding to the wheels in contact with the ground were fixed, while the suspended wheel remained free. The weight of the chassis and components was applied by distributed forces over the upper part of the frame. As can be seen in the strain distribution diagram in Figure 4, the maximum strain under this condition is 3.2336 mm, concentrated in the area opposite the raised wheel. According to the stress distribution shown in Figure 5, when the car is fully loaded and with one front wheel suspended, the maximum stress is 93.666 MPa. Compared to the allowable limits of the material, there is still a significant strength margin, meeting the system requirements.

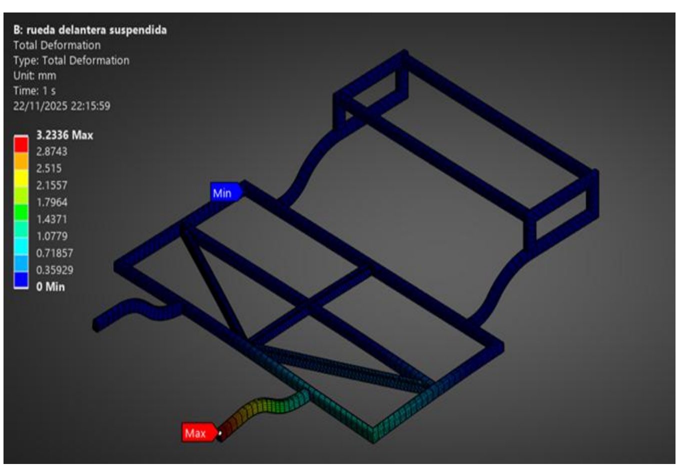

Fig. 4 Equivalent displacement diagram of the frame structure.

D. Static analysis of the chassis where one side of the rear wheel is suspended under full load

This simulation evaluated the chassis response when a rear wheel loses contact with the ground, generating an asymmetric stress on the structure. The total load and support conditions remained the same as in the previous case, adapting the restraint according to the position of the raised wheel.

The application of the vehicle's own weight and external loads was achieved through gravity and distributed forces on the upper part of the frame. As can be seen in the strain distribution diagram in Figure 6, the maximum strain under this condition is 1.5483 mm, concentrated in the rear area of the raised opposite wheel. According to the stress distribution shown in Figure 7, when the vehicle is fully loaded and with one rear wheel suspended, the maximum stress is 130.71 MPa.

The results showed increased deformation in the rear section, with stress concentrations at the longitudinal member joints. However, the values remained within acceptable limits, confirming the structural stability of the chassis under rear torsion conditions.

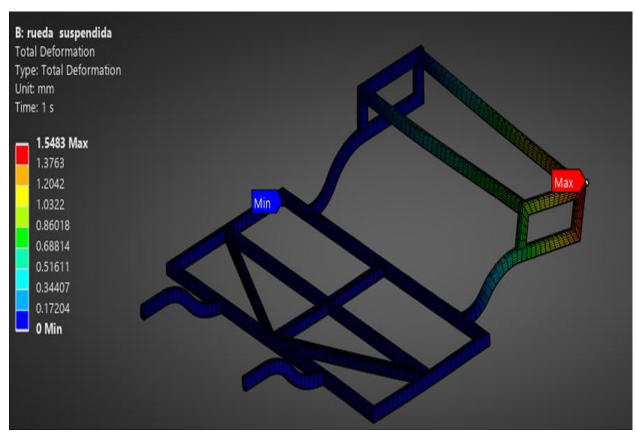

Fig. 6 Equivalent displacement diagram of the frame structure.

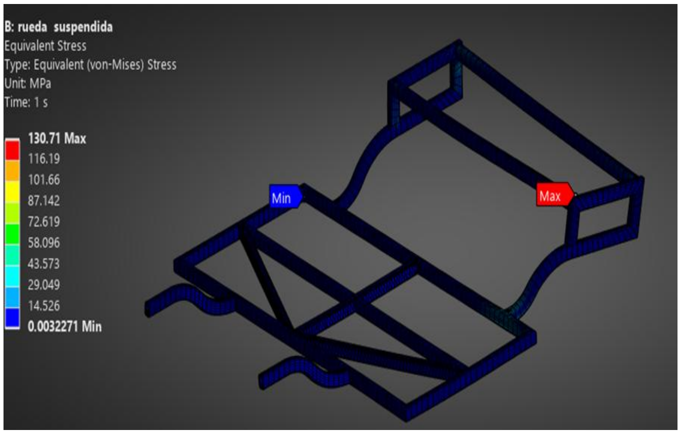

Fig. 7 Equivalent stress diagram (Von Mises).

E. Analysis of emergency braking under full load conditions

Under this condition, the chassis response to sudden braking was evaluated, considering the total system load and a dynamic factor of 1.5. A uniform deceleration was applied along the vehicle's longitudinal axis to simulate the inertia produced by braking. Supports were assigned to the wheel contact areas, while loads were distributed over the main structure. As can be seen in the strain distribution diagram in Figure 8, the maximum strain under this condition is 0.86547 mm. According to the stress distribution shown in Figure 9, when the vehicle is fully loaded, the maximum stress is 136.04 MPa.

The results showed that the highest stresses are concentrated in the front of the chassis, where most of the braking force is transmitted. Even so, the deformations obtained remained within the elastic range, ensuring that the frame can withstand emergency braking maneuvers without compromising its structural integrity..

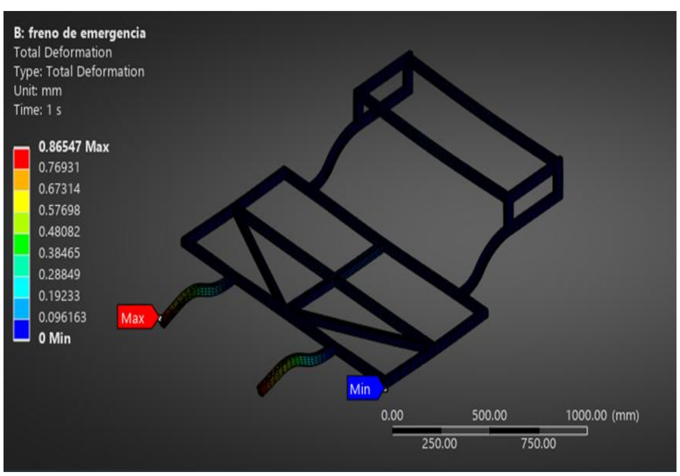

Fig. 8 Equivalent displacement diagram of the frame structure.

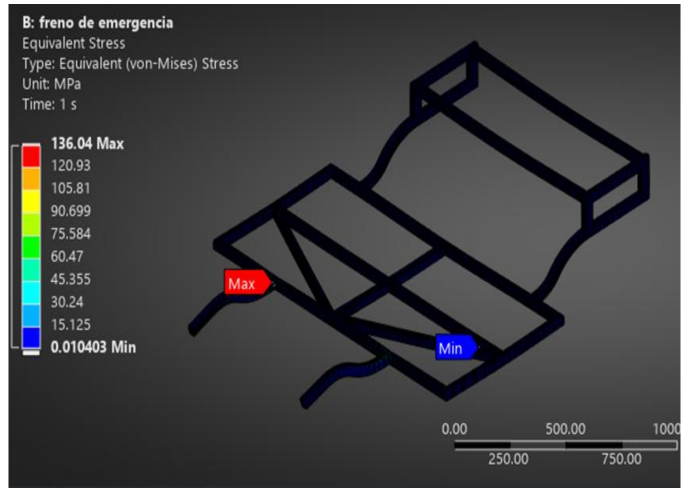

Fig. 9 Equivalent stress diagram (Von Mises)

Table III summarizes the results obtained in the four scenarios evaluated during the structural analysis of the chassis. It includes the maximum deformation and equivalent stress (Von Mises) values recorded for each simulated condition, allowing for a comparison of the design's performance under static, torsional, and dynamic loads.

TABLE III
STRESS AND STRAIN DATA FOR EACH WORKING CONDITION FOR STEEL

Working conditions	Four wheels on the ground	Suspended front wheel	Suspended rear wheel	Emergency braking
Maximum displacement (mm)	0.57543	3.2336	1.5483	0.86547
Maximum stress (MPa)	45.099	93.666	130.71	136.04

The values show that the suspended wheel condition generates the greatest deformation, while braking presents the highest stress concentration. However, in neither case is the material's elastic limit exceeded, confirming that the design maintains an adequate margin of structural safety.

STRUCTURAL COMPARISON OF MATERIALS

For the comparison between structural steel, aluminum, and Q345 steel, the same chassis geometry was maintained in all cases in order to evaluate only the influence of the material properties. All simulations were performed using a rectangular tubular profile of 50 mm × 30 mm with a wall thickness of 5 mm, keeping the same overall chassis dimensions, boundary conditions, loads, and mesh. Under this approach, the cross-section, thickness, and profile type (rectangular tubular) were not modified. The difference between the analyzed cases is reflected in the total weight of the structure, which is approximately 50 kg for structural steel and Q345, while for aluminum, due to its lower density, the chassis weight is reduced to approximately 40 kg. The lower equivalent Von Mises stress values obtained for aluminum are attributed to its lower elastic modulus, which results in higher deformations and a more uniform redistribution of internal forces, reducing stress concentrations but leading to lower global stiffness.

TABLE IV

MAXIMUM EQUIVALENT DISPLACEMENTS OBTAINED FOR EACH MATERIAL IN THE FOUR SIMULATED SCENARIOS

Working conditions	Steel	Aluminum	Q345
Four wheels on the ground (mm)	0.57543	1.75131	0.57543
Suspended front Wheel (mm)	3.23360	**9.84139**	3.23360
Suspended rear Wheel (mm)	1.54830	4.71222	1.54830
Emergency braking (mm)	0.86547	2.63404	0.85547

The results in Table IV show that steel and Q345 exhibit virtually identical deformations, significantly lower than those of aluminum, reflecting greater torsional stiffness and structural stability. Aluminum, due to its lower modulus of elasticity, shows greater displacements, although without exceeding permissible limits, making it a viable alternative if the geometric design is optimized or the profile thickness is increased. Subsequently, equivalent stresses (Von Mises) are analyzed, allowing for the evaluation of the material's resistance to the same applied loads.

TABLE V

MAXIMUM EQUIVALENT STRESSES OBTAINED FOR EACH MATERIAL IN THE FOUR SIMULATED SCENARIOS.

Working conditions	Steel	Aluminum	Q345
Four wheels on the ground (MPa)	45.099	14.818	45.06
Suspended front Wheel (MPa)	93.666	30.776	93.63
Suspended rear Wheel (MPa)	130.710	42.948	130.68
Emergency braking (MPa)	136.040	44.699	134.01

Table V shows that, although aluminum experiences greater deformation, it operates under lower stresses due to the internal redistribution caused by its lower stiffness. Steel and Q345, on the other hand, maintain stresses well below their elastic limits, even under critical conditions such as a suspended wheel or emergency braking, offering a greater margin of structural safety. The results indicate that material selection must balance the stiffness-weight-strength ratio. Structural steel and Q345 steel excel when maximum structural stability, resistance to dynamic loads, and torsional stiffness are prioritized. Aluminum, while less stiff, offers a significant weight advantage, which can improve energy efficiency in electric vehicle applications, provided a reinforced or optimized design is implemented.

IV. DISCUSSION AND IMPROVEMENT

The results of the structural analysis show that the chassis performs adequately to the four evaluated conditions. Under static load with all four wheels on the ground, stresses and strains were low, indicating good overall stiffness. In cases with one wheel suspended (front and rear), the structure experienced greater deformations due to the asymmetric load, although the values obtained remained within the material's elastic range. Finally, under emergency braking, the greatest stress concentration was observed in the front area, but without exceeding the yield strength. Based on these results, the possibility of improving torsional stiffness and stress distribution is identified. One viable improvement consists of reinforcing critical areas by increasing local thickness or by using circular tubular profiles to replace rectangular sections in areas subjected to torsion. Another option could be the use of a different, more suitable material.

V. CONCLUSIONS

The structural analysis performed verified that the chassis meets the established mechanical requirements for the four evaluated conditions. In all cases, the obtained stresses and deformations remained within the elastic range of the material, confirming that the design presents an adequate safety margin and stable behavior under real operating loads. The proposed chassis exhibits a strong and reliable structural response under the analyzed loading conditions.

The simulations showed that asymmetric loading conditions represent the most critical structural scenario for the chassis, particularly when one wheel loses contact with the ground. Nevertheless, the maximum stress values obtained did not exceed the yield strength of the material, demonstrating adequate torsional rigidity and structural integrity.

The results also allow the identification of improvement opportunities through localized geometric optimization. Design modifications such as increasing the thickness in high-stress regions or replacing rectangular tubular profiles with circular sections could further enhance torsional strength without significantly increasing the overall weight of the structure.

REFERENCES

[1] Bahatmaka, A., Maulana, A.Y., Amin, M., Pratama, F.R.S., Prabowo, A.R., Fitriyana, D.F., Seo, H.A., Ju, H., and Cho, J.H.: Material performance analysis in frontal collision simulation of electric vehicle frames using explicit dynamic finite element analysis method, Results in Engineering, 28, 107130,https://doi.org/10.1016/j.rineng.2025.107130, 2025.

[2] Capata, R., Martellucci, L., Buccolini, D., de Felice, C., and Giannini, M.: Validation Method of Torsional Stiffness for a Single-Seater Car Chassis, World Electric Vehicle Journal,16,604,https://doi.org/10.3390/wevj16110604, 2005.

[3] Ding, R., Qi, X., Meng, X., Chen, X., Zhang, L., Mei, Y., Li, A., and Ye, Q.: A Review on the Chassis Configurations and Key Technologies of Agricultural Robots, Agriculture (Switzerland), 15, 2379, https://doi.org/10.3390/agriculture15222379, 2025.

[4] Feng, J., Chen, W., Liu, C., Tan, P., Liu, K., and Zhou, Z.: Work-phase recognition in construction machinery using gated recurrent unit with attention and fractional calculus features, Computer-Aided Civil and Infrastructure Engineering, 40, 4904–4928, https://doi.org/10.1111/mice.70091, 2025.

[5] Freddi, M., Pagliari, C., and Frizziero, L.: Parametric Sensitivity Analysis of Suspension Design Using Response Surface Techniques, Applied Sciences (Switzerland), 15,11887,https://doi.org/10.3390/app152211887, 2025.

[6] Guan, S., Wang, A., Wang, H., Liu, Z., and Hou, S.: Fatigue life prediction of rubber bushings under multiaxial random loads based on the rainflow counting method, Results in Engineering,28,107294,https://doi.org/10.1016/j.rineng.2025.107294, 2025.

[7] Guo, J., Wang, S., Guo, Z., Pan, J., Wang, G., Chen, Z., Liu, Z., Wu, S., and Guan, W.: Dynamic characteristics analysis and optimization of track-soil interaction based on DEM-MBD coupling method, Powder Technology, 468, 121678, https://doi.org/10.1016/j.powtec.2025.121678, 2026.

[8] Meng, D., Guan, C., Li, W., Liang, J., and Zhang, L.: Nonlinear dynamic modeling and analysis of steering brake squeal considering the deflection effect of friction pairs, Nonlinear Dynamics, 113, 32117–32138, https://doi.org/10.1007/s11071-025-11788-8, 2025.

[9] Meng, Z., Wang, D., Lian, F., Dong, J., Ni, Y., Cao, X., Wang, C., and Chen, L.: Structure–material–performance integrated intelligent lightweight optimization of truck frames, Structural and Multidisciplinary Optimization,68,247,https://doi.org/10.1007/s00158-025-04199-1, 2025.

[10] Millan, P. and Ambrósio, J.: On the Effect of the Stiffness of the Body-in-White in the Dynamics of a Vehicle Flexible Multibody Model, Mechanisms and Machine Science, 195, 70–82, https://doi.org/10.1007/978-3-032-10862-3_7, 2026.

[11] Namasivayam Sukumaar, V., Ishak, M.R., Abdullah, M.N., Mohd Zuhri, M.Y., and Rizal, M.A.: Investigation of flexural mechanical and creep properties of sleeve reinforced pultruded glass fibre reinforced polymer composite for crossarm application, Scientific Reports, 15, 16023, https://doi.org/10.1038/s41598-025-00732-w, 2025.

[12] Sun, X., Sun, W., Lv, S., Luo, H., Ni, C., Zhang, Y., and Zhang, H.: Dynamic modeling and frequency veering analysis of carbon-fiber-reinforced-composite C-shaped rod, International Journal of Mechanical Sciences,307,110932,https://doi.org/10.1016/j.ijmecsci.2025.110932, 2025.

[13] S. Capata, L. Martellucci, D. Buccolini, C. de Felice, and M. Giannini, "Validation method of torsional stiffness for a single-seater car chassis," World Electric Vehicle Journal, vol. 16, no. 11, p. 604, 2005, https://doi.org/10.3390/wevj16110604.

[14] Tomasi, I., Grandi, S., Donzella, G., and Solazzi, L.: Implementation of Composite Materials for Lightweighting of Industrial Vehicle Chassis, Journal of Composites Science,9,611,https://doi.org/10.3390/jcs9110611, 2025. Wakshume, E.: Lightweight composite optimization of URAL-4320 chassis using CFRP and BFRP: Structural and modal finite element analysis, Results in Engineering, 28, 108134,https://doi.org/10.1016/j.rineng.2025.108134, 2025.

[15] Wang, Y., Chen, W., Gu, C., and Meng, H.: Suppressing Vehicle Shimmy Based on Inerter-based Nonlinear Damping Dissipation Mechanism, Journal of Vibration Engineering and Technologies, 13, 615, https://doi.org/10.1007/s42417-025-02183-z, 2025.

[16] Widyianto, A., Budiman, Y., Anugrah, R.A., Fatin, N.N., and Wibowo, H.: Optimizing enhanced smart architecture frame (eSAF) topology: A computational approach to weight and strength trade-offs, Results in Engineering,28,107614,https://doi.org/10.1016/j.rineng.2025.107614, 2025.

[17] Yan, K., Hu, Z., Zhang, X., Li, J., Xu, L., and Ouyang, M.: A multimodal surrogate model for the multiphysics optimization of dual-rotor in-wheel motors, Advanced Engineering Informatics, 69, 103816, https://doi.org/10.1016/j.aei.2025.103816, 2026.

[18] Zamzam, O., Ramzy, A.A., Abdelaziz, M., Elnady, T., and Abd El-Wahab, A.A.A.: Structural performance evaluation of electric vehicle chassis under static and dynamic loads, Scientific Reports, 15, 5168, https://doi.org/10.1038/s41598-025-86924-w, 2025.

[19] Zhang, B., Wang, X., Dai, S., Zhang, Y., Tan, C.A., and Li, S.: Fourier-Laplace based semi-analytical solution and optimization for vehicle and infinite-length road interaction, Mechanical Systems and Signal Processing,243,113689,https://doi.org/10.1016/j.ymssp.2025.113689, 2026.

[20] Zhang, Z., Wang, D., Chen, H., Zhang, S., and Chen, J.: Multi-condition combined topology optimization design of electric truck aluminum alloy frame based on subjective and objective interactive weights, Proceedings of the Institution of Mechanical Engineers, Part D: Journal of Automobile Engineering, 239, 7480–7493, https://doi.org/10.1177/09544070241301189, 2025.